Published online 21 November 2010 *Nucleic Acids Research, 2011, Vol. 39, No. 6* ***2319–2329***
doi:10.1093/nar/gkq1164

Stoichiometry and affinity for thymine DNA glycosylase binding to specific and nonspecific DNA

Michael T. Morgan, Atanu Maiti, Megan E. Fitzgerald and Alexander C. Drohat*

Department of Biochemistry and Molecular Biology and Greenebaum Cancer Center, School of Medicine, University of Maryland, Baltimore, MD 21201, USA

Received August 6, 2010; Revised October 12, 2010; Accepted October 31, 2010

ABSTRACT

Deamination of 5-methylcytosine to thymine creates mutagenic G·T mispairs, contributing to cancer and genetic disease. Thymine DNA glycosylase (TDG) removes thymine from these G·T lesions, and follow-on base excision repair yields a G·C pair. A previous crystal structure revealed TDG (catalytic domain) bound to abasic DNA product in a 2:1 complex, one subunit at the abasic site and the other bound to undamaged DNA. Biochemical studies showed TDG can bind abasic DNA with 1:1 or 2:1 stoichiometry, but the dissociation constants were unknown, as was the stoichiometry and affinity for binding substrates and undamaged DNA. We showed that 2:1 binding is dispensable for G·U activity, but its role in G·T repair was unknown. Using equilibrium binding anisotropy experiments, we show that a single TDG subunit binds very tightly to G·U mispairs and abasic (G·AP) sites, and somewhat less tightly G·T mispairs. Kinetics experiments show 1:1 binding provides full G·T activity. TDG binds undamaged CpG sites with remarkable affinity, modestly weaker than G·T mispairs, and exhibits substantial affinity for nonspecific DNA. While 2:1 binding is observed for large excess TDG concentrations, our findings indicate that a single TDG subunit is fully capable of locating and processing G·U or G·T lesions.

INTRODUCTION

A large percentage of point mutations in cancer and genetic disease are C→T transitions at CpG sites, resulting largely from replication of G·T mispairs created by deamination of 5-methylcytosine (m^5C) to thymine (1–4). Thymine DNA glycosylase (TDG) is charged with finding these G·T lesions and removing thymine to initiate base excision repair, which ultimately restores a G·C base pair (5,6). Methyl binding domain IV (MBD4) is another DNA glycosylase that processes G·T mispairs arising from m^5C deamination at CpG sites (7,8). About 4% of cytosines in mammalian DNA are methylated, selectively at CpG sites, and this key modification promotes transcriptional silencing and is essential for many cellular processes and for embryonic development (9). It is known that cytosine 5-methyltransferases catalyze the conversion of C to m^5C at CpG sites in DNA, but the mechanism for 'demethylation' of m^5CpG has remained elusive (9). Several recent studies indicate a BER-mediated pathway for active demethylation (10,11); many indicate a mechanism for active m^5C deamination, giving a G·T mispair that could be processed by TDG (or MBD4) and BER to restore a G·C pair (12–16). A preliminary report that inactivation of TDG causes embryonic lethality in mice (17), the first such finding for any DNA glycosylase, is consistent with an essential role for TDG in transcriptional regulation, in addition to processing G·T mispairs arising from spontaneous m^5C deamination.

Given the critical role of TDG in protecting against C→T mutations and its emerging role(s) in transcriptional regulation, it is important to obtain a detailed understanding of how TDG recognizes and processes lesions, how its activity is stimulated by the follow-on BER enzyme, APE1 and to characterize its interaction with undamaged CpG sites and nonspecific DNA. Our recent crystal structure of TDG (catalytic domain) bound to abasic DNA (18) revealed a remarkable 2:1 complex, with one TDG subunit bound at the abasic site and an adjacent subunit bound to undamaged DNA (Figure 1). Such 2:1 binding had not previously been observed for TDG, MUG or UNG. Our previous biochemical studies showed TDG, full length and catalytic domain, can bind abasic DNA with 1:1 or 2:1 stoichiometry, depending on TDG concentration (18). However, the affinity for each TDG subunit (K_{d1} and K_{d2}) remained unknown. Determining these values is important for understanding the catalytic mechanism of TDG and how its activity is stimulated by APE1, i.e.

*To whom correspondence should be addressed. Tel: +1 410 706 8118; Fax: +1 410 106 8297; Email: adrohat@som.umaryland.edu

how the first steps of BER are coordinated. In addition, the stoichiometry for binding G•T or G•U substrates had not been examined. Although we previously showed 1:1 binding provides full catalytic activity for G•U lesions (18), TDG exhibits much weaker binding and catalysis for G•T relative to G•U substrates (19–22), raising the question of whether 2:1 binding could be needed for efficient G•T repair. This is important, because G•T lesions are considered the predominant biological substrate for TDG (21,23). Our previous studies demonstrate TDG can excise bulky cytosine analogs from a CpG site in DNA (24), suggesting TDG may have substantial affinity for undamaged CpG sites, but this had not been determined. Additionally, previous studies suggest TDG possesses significant affinity for nonspecific DNA (25), but this has not been quantitatively examined. Determining the affinity and stoichiometry of TDG for binding CpG sites and nonspecific DNA is important for understanding its functions in DNA repair and transcriptional regulation. We address these important questions here using pre-steady-state kinetics and equilibrium binding experiments.

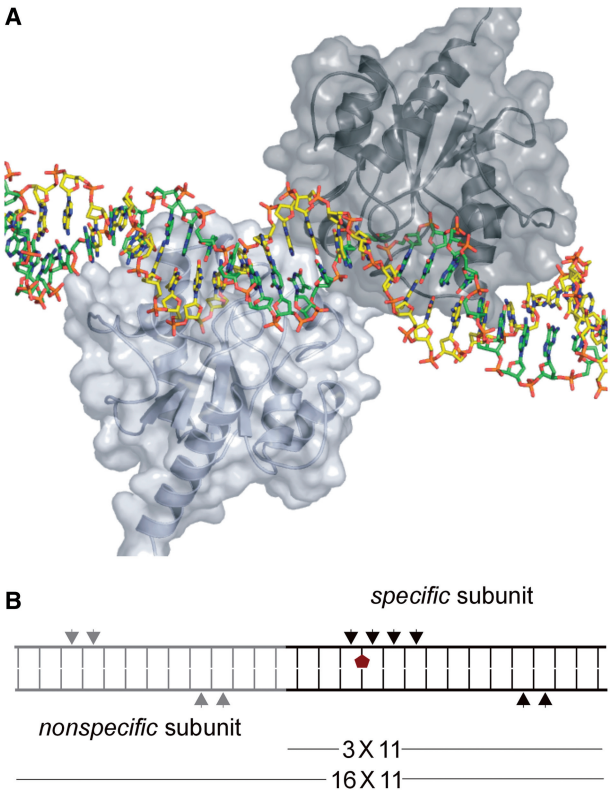

Figure 1. TDG can form a 2:1 complex with DNA. (**A**) Our previous crystal structure shows TDG (catalytic domain) can form a 2:1 complex with abasic DNA, one subunit (dark gray) binds the flipped abasic nucleotide and the adjacent subunit (light gray) binds to undamaged DNA. The protein–protein interface buries ~300 Å^2 of accessible surface area per subunit. (**B**) Cartoon depicting the contacts to DNA phosphates made by the specific TDG subunit (black triangles) and the nonspecific subunit (gray triangles) with respect to the lesion site (red). The DNA constructs used for the studies reported here are 16X11 (28 bp) and 3X11 (15 bp), where X represents the target nucleotide (Figure 2). The 16X11 DNAs can accommodate 2:1 binding as observed in the crystal structure, but the 3X11 DNAs cannot.

MATERIALS AND METHODS

DNA synthesis and purification

The DNA used for this work is shown in Figure 2. Duplex DNA was hybridized by rapid heating to 80°C followed by slow cooling to room temperature. DNA oligonucleotides were synthesized at the Keck Foundation Biotechnology Resource Laboratory of Yale University (trityl-on), purified using Glen-Pak purification cartridges (Glen Research), and quantified by absorbance (260 nm) as described (22,24). Purity was verified by analytical anion-exchange high-performance liquid chromatography (HPLC) under denaturing (pH 12) conditions (24).

The oligonucleotides containing substrate analogs 2′-deoxy-2′-flouroarabinothymidine (T^F, Figure 2) or 2′-deoxy-2′-flouroarabinouridine (U^F) were obtained as described (22). Control experiments demonstrate DNA containing U^F or T^F is completely resistant to cleavage by TDG (saturating concentration) for >48 h, consistent with previous findings for TDG (26) and MUG (27). Previous studies and our findings here indicate T^F and U^F are excellent mimics of dT and dU, and do not significantly perturb the structure of B-type DNA (22,26–29).

The DNA used for fluorescence anisotropy experiments was labeled with sulphorhodamine (Texas Red, TR) in the non-target strand (5′ amino C6 modifier), and was

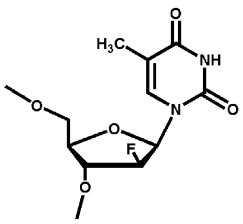

2′-deoxy-2′-fluoroarabinothymidine (T^F)

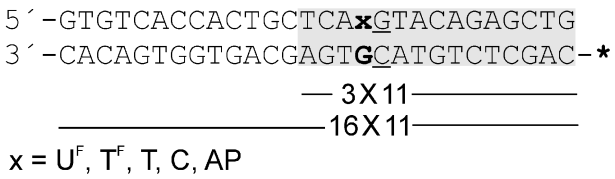

Figure 2. DNA used in this work. We used two non-cleavable substrate analogs, 2′-deoxy-2′-flouroarabinothymidine (T^F) and 2′-deoxy-2′-flouroarabinouridine (U^F) to monitor TDG binding to substrate in the absence of base excision. Two DNA constructs were used; 16X11 can accommodate 2:1 binding as seen in the crystal structure, while 3X11 cannot (Figure 1). The target nucleotide (x = U^F, T^F, AP, T or C) is paired with guanine (bold) and placed in a CpG dinucleotide context, in keeping with the specificity of TDG. The DNA contains no other CpG site. The DNA was labeled at the 5′ end of the non-target strand (*) with sulforhodamine (also called Texas Red or TR) for anisotropy experiments or with fluorescein for EMSAs. The 28 bp nonspecific DNA (NS28) contains no mispair or CpG site.

synthesized and purified (RP-HPLC) by the Midland Certified Reagent Co. (Midland, TX, USA).

Abasic (AP) DNA was generated by incubating 16U11 or 3U11 (2000 nM) with a 1000-fold lower concentration (2 nM) of uracil DNA glycosylase (UNG) at 23°C for 30 min, sufficient time for complete conversion of substrate to abasic product (16AP11 or 3AP11), and used immediately for anisotropy or electrophoretic mobility shift assay (EMSA) experiments. After dilution of AP DNA (4000-fold) to the concentration used for anisotropy (0.5 nM), the residual UNG (0.0005 nM) is far too dilute to bind the AP DNA ($K_d > 15$ uM) (30) or effect the binding of TDG. Although the higher AP–DNA concentration used for EMSA (0.5 μM) resulted in a higher residual UNG concentration (0.5 nM), given its weak affinity for AP DNA, and the 1000-fold excess concentration of AP DNA, UNG will have no effect on TDG binding.

Enzyme purification

Human thymine DNA glycosylase (TDG) was expressed and purified as described (18,21), flash frozen, and stored at −80°C. The enzyme concentration is determined by absorbance, using a molar absorption coefficient of $\varepsilon^{280} = 31.5\,mM^{-1}\,cm^{-1}$, measured using the Edelhoch method, as described (31). We typically find TDG is fully active, as indicated by observation that for pre-steady-state multiple turnover kinetic experiments collected for G•U and G•FU substrates, the amplitude of the exponential phase is equal to the TDG concentration, (Supplementary Figures S1 and S2).

Kinetics experiments

We used single turnover kinetics experiments under saturating enzyme conditions ($[E] > [S] >> K_d$) to obtain a rate constant (k_{max}) that is not influenced by product release or product inhibition. This is important because TDG exhibits very slow product release and strong product inhibition, which dominates k_{cat} values determined using steady-state kinetics (19,32,33). Experiments were collected at room temperature (23°C) in HEMN.1 buffer (0.02 M HEPES, 0.2 mM EDTA, 2.5 mM $MgCl_2$, 0.1 M NaCl). Experiments were initiated by adding concentrated TDG to buffered substrate, followed by rapid mixing. At various time points, aliquots were removed, quenched with 50% (v:v) 0.3 M NaOH and 0.03 M EDTA, and heated at 85°C for 15 min to cleave the DNA backbone at enzyme-produced abasic sites. The fraction product was determined by HPLC (21,24). The data were fitted to Equation (1) using nonlinear regression with Grafit 6 (34):

$$\text{fraction product} = A(1 - e^{-kt}) \quad (1)$$

where A is the amplitude, k is the rate constant and t is the reaction time (min). The DNA substrate concentration was 0.5 μM, and the TDG concentration, 5 μM, was nearly 300-fold higher than the K_d for G•T substrate binding determined here (see below). These saturating enzyme conditions provide the maximal rate constant for product formation ($k \approx k_{max}$).

We also determined the maximal rate of product formation using kinetics experiments as described above, but with saturating substrate conditions ($[S] >> K_d$, and $[S] >> [E]$) (22,33). The data were fitted to Equation (2) using nonlinear regression with Grafit 6:

$$\text{product (nM)} = A(1 - e^{-kt}) + vt \quad (2)$$

where A and k are the amplitude and rate constant of the exponential phase, v is steady-state velocity and t is time. The steady-state rate constant (k_{cat}) is calculated by dividing steady-state velocity by enzyme concentration.

Fluorescence anisotropy experiments and data fitting

Equilibrium binding of TDG to DNA was studied by fluorescence anisotropy using a QuantaMaster 40 spectrofluorometer (PTI), monitoring the fluorescence of sulphorhodamine (Texas Red, or TR) conjugated to the 5′-end of the non-target strand (Figure 2). Previous studies show the benefits of using X-rhodamine or sulphorhodamine for monitoring protein nucleic acid interactions by fluorescence anisotropy (35–37). TDG was titrated into HEMN.1 buffer (above) that contained TR-labeled DNA, supplemented with 1% glycerol and 1 uM BSA. The DNA concentration was maintained at a fixed value throughout the titration by adding concentrated enzyme in buffer that also contained DNA. After each addition of TDG, the sample was incubated for at least 2 min before data collection to ensure binding was at equilibrium. This was confirmed by observation that the anisotropy was constant for at least 5 min (for some data points). Anisotropy data were collected in T-format, where one PMT is connected directly to the sample compartment (no monochromator) with wavelength selection provided by a 628-nm band pass filter (Semrock, Inc.). The excitation wavelength was 590 nm (3-nm band pass) and the single-emission monochromator was set to 615 nm (5-nm band pass). Wavelength selection for the monochromators was enhanced with 586 and 624 nm band-pass filters (Semrock, Inc.) for excitation and emission, respectively.

The equilibrium dissociation constants for TDG binding to TR-labeled DNA were determined by fitting the fluorescence anisotropy data to appropriate models using DynaFit 4 (38,39). The models and DynaFit scripts used for data fitting are given in the Supplementary Data. The fitted parameters included dissociation constants for one or two binding sites on the DNA, and anisotropy values for free DNA (r_D) and for 1:1 and 2:1 complexes with TDG (r_{ED} and r_{EED}). In many cases, the data clearly indicate two nonequivalent binding sites. Model discrimination was also informed by the probability value of the Fisher's F-statistic, obtained from data fitting, where $P < 0.05$ is considered significant. The reported parameters are derived from global fitting of at least two independent binding experiments. We determined the equilibrium dissociation constant for TDG binding to unlabeled DNA using equilibrium competition anisotropy experiments, where TDG binding to TR-labeled $16U^F11$ was monitored in the presence of varying concentrations of unlabeled DNA. DynaFit was used for global fitting of the data to a model involving one or two TDG binding sites for the

unlabeled DNA and two binding sites for TR-labeled 16U^{F}11. A benefit of using DynaFit for the data presented here is that data fitting does not require an analytical equation, which could involve assumptions that are not compatible with experimental restraints. Indeed, the standard model for two nonequivalent binding sites assumes the species being monitored (DNA) is present at much lower concentration than the dissociation constant. This is not feasible for monitoring TDG binding to 16U^{F}11, because the minimal DNA concentration needed for sufficient sensitivity in the anisotropy experiment (0.5 nM) approximates the dissociation constant (K_{d1} = 0.6 nM, see below).

Electrophoretic mobility shift assays

EMSAs were performed, essentially as described (18), to provide an independent method for determining the stoichiometry of TDG–DNA complexes. The EMSAs were performed with precast 6% polyacrylamide native gels (Invitrogen) and analyzed using a Typhoon 9400 imager (GE Healthcare).

RESULTS

Experimental approach

We used fluorescence anisotropy and EMSAs to determine the affinity and stoichiometry for TDG binding to DNA containing a U^F or a T^F substrate analog, an abasic (or AP) site, an undamaged CpG site, and nonspecific DNA. We and others have shown the U^F and T^F analogs are excellent mimics of the natural dU and dT substrates, because they allow formation of the catalytically competent enzyme–substrate complex in the absence of base excision (22,26,27,29). The U^F and T^F analogs differ from dU and dT only by replacement of 2′-H with fluorine (2′-fluoro-*arabino*, Figure 2), which renders the base-sugar (*N*-glycosylic bond) of these and other nucleotides highly resistant to spontaneous and enzymatic cleavage. Previous studies show the 2′-fluoroarabino substitution, in dT and other deoxynucleotides, promotes an O4′-*endo* sugar pucker (rather than C2′-*endo*), which is fully compatible with B-DNA geometry (28,40,41). Although the O4′-*endo* conformation in a substrate analog could potentially alter the binding of a DNA glycosylase, our previous studies indicate the effect is small for TDG binding to DNA containing a T^F analog (22).

Our studies employed two different DNA lengths (Figure 2), one that can accommodate 2:1 binding as observed in the TDG AP–DNA crystal structure (16X11, X = target nucleotide) and a shorter construct (3X11) that lacks the nonspecific binding site seen in the crystal structure (Figure 1). For all DNAs used here, the target base is paired with guanine (i.e. G•T^F), in keeping with the specificity of TDG (19,21).

For the fluorescence anisotropy experiments, the DNA was labeled with sulphorhodamine (Texas Red, TR) as indicated in Figure 2. Previous studies indicate sulphorhodamine and X-rhodamine are well suited for characterizing protein–DNA interactions (35–37,42,43). When conjugated to DNA, these fluorophores are bright and typically exhibit fluorescence decay that is dominated by a single lifetime and relatively independent of conditions and protein binding, and their anisotropy is strongly correlated with DNA rotation, with minimal contribution from independent fluorophore mobility. These properties are highly desirable for studying protein–DNA interactions, particularly for complex binding mechanisms as shown below for TDG.

TDG binding to a G•U mispair

We first consider equilibrium binding of TDG to 16U^{F}11, which is long enough to accommodate 2:1 binding as observed in the TDG•AP–DNA crystal structure (Figure 3A). As shown in Figure 3B, the fluorescence anisotropy data clearly indicate two nonequivalent binding sites, and fitting to a two-site model reveals a huge difference in affinity, $K_{d1} = 0.63 \pm 0.16$ nM and $K_{d2} = 662 \pm 108$ nM (Table 1). Thus, TDG forms a very tight 1:1 complex with the G•U^F site, and a second TDG subunit binds with 1000-fold weaker affinity to give a 2:1 complex at high TDG concentrations. TDG binding to 16U^{F}11 was qualitatively assessed using an EMSA, which confirms the binding stoichiometry indicted by the anisotropy data (Figure 3C).

We also examined TDG binding to 3U^{F}11, a DNA construct which lacks the entire binding site for the second TDG subunit of the 2:1 complex, as seen in the crystal structure (Figure 1. The anisotropy data show TDG forms a tight 1:1 complex with the G•U^F site of 3U^{F}11, $K_{d1} = 8.4 \pm 2.9$ nM, and a second TDG subunit can bind with very weak affinity, $K_{d2} = 2650 \pm 463$ nM (Figure 3D). The results of an EMSA confirm this binding stoichiometry (Figure 3E). Although 2:1 binding to 3U^{F}11 is observed at high TDG concentrations, the second subunit must bind an alternate site from that seen in the crystal structure, as discussed below. Kinetics experiments show this alternate 2:1 complex does not contribute to G•U binding or processing, because catalytic activity is nearly the same for conditions that give 2:1 binding (saturating TDG) or 1:1 binding (saturating substrate, Supplementary Figure S.2). The finding that TDG binds tightly to 3U^{F}11 shows the 2:1 complex observed in the crystal structure is not required for specific recognition of a G•U lesion, consistent with previous kinetics experiments showing 2:1 binding is not needed for full G•U catalytic activity (18).

A number of observations suggest the alternate 2:1 complex for 3U^{F}11 (and other 3X11 DNAs) involves transient and nonspecific binding of the catalytic domain and/or the N-terminal region of TDG to DNA, and perhaps some degree of protein-protein interactions. Sedimentation velocity experiments show TDG is predominantly a monomer at concentrations of 20 and 50 μM (Supplementary Figure S3). This indicates the alternate 2:1 complex, with $K_{d2} = 2.7$ μM (for 3U^{F}11), is not comprised solely of protein–protein interactions (though such interactions might be enhanced for DNA-bound TDG). Previous studies show the disordered N-terminal domain of TDG (residues 1–120) forms nonspecific interactions with DNA (25,44), which may contribute to the

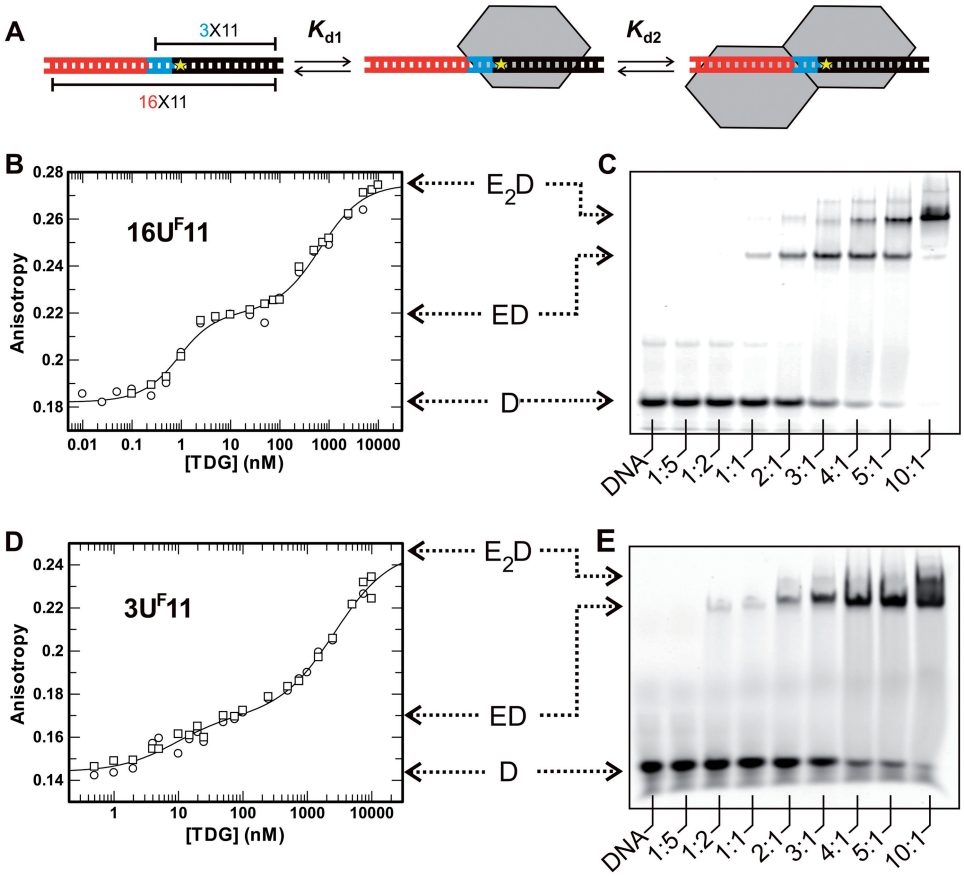

Figure 3. TDG binding to G•U^F substrate analogs monitored by fluorescence anisotropy and EMSA. (**A**) Model for sequential 2:1 binding of TDG to two different sites on a 28 bp DNA with a 16X11 construct. (**B**) Anisotropy data for equilibrium binding of TDG to the 16U^{F}11 substrate analog (0.5 nM), obtained from two independent experiments (open circle, open rectangle). Fitting the data to a two-site binding model using DynaFit 4 gives K_{d1} = 0.63 ± 0.16 nM and K_{d2} = 662 ± 108 nM, and anisotropy values of r_D = 0.182, r_{ED} = 0.220, r_{EED} = 0.275. (**C**) EMSA for TDG binding to 16U^{F}11 (0.5 uM), with the [TDG]:[DNA] ratio indicated. Arrows indicate anisotropy values or gel bands corresponding to free DNA (D), the 1:1 complex (ED), and the 2:1 complex (EED). (**D**) Anisotropy data for TDG binding to the 3U^{F}11 analog (0.5 nM) from two independent experiments (open circle, open rectangle). Fitting to a two-site binding model gives K_{d1} = 8.4 ± 2.9 nM and K_{d2} = 2650 ± 463 nM (and r_D = 0.144, r_{ED} = 0.170, r_{EED} = 0.247). (**E**) EMSA for TDG binding to 3U^{F}11 (0.5 uM).

Table 1. Equilibrium dissociation constants for TDG binding to specific and nonspecific DNA

DNA	K_{d1} (nM)	K_{d2} (nM)	K_{d2}/K_{d1}
16U^{F}11	0.63 ± 0.16	662 ± 108	1051
3U^{F}11	8.4 ± 2.9	2650 ± 463	315
16T^{F}11	18 ± 3	1279 ± 279	71
3T^{F}11	124 ± 25	818 ± 80	7
16AP11	1.4 ± 0.4	1926 ± 762	1376
3AP11	6.2 ± 1.3	3480 ± 1173	561
16C11	63 ± 10	965 ± 148	15
NS28[a]	293 ± 64	1172 ± 254	4[a]

[a]Parameters obtained from equilibrium competition experiments fitted to a model for two equivalent and independent binding sites (restrained to $K_{d2} = 4*K_{d1}$).

alternate 2:1 complex. Consistent with this, K_{d2} is much weaker for the catalytic domain (TDG-core, 111–308), which binds 3U^{F}11 with K_{d1} = 83 ± 46 nM and K_{d2} = 21 ± 3 μM (Supplementary Figure S4). Previous sedimentation velocity experiments show TDG-core is fully monomeric at 120 μM (18). Thus, K_{d2} = 21 μM for TDG-core binding to 3U^{F}11 suggests the catalytic domain also exhibits nonspecific DNA interactions, because DNA binding seems unlikely to promote protein–protein interactions for TDG-core (18,45). Although the detailed nature of the alternate 2:1 complex is not presently clear, it only arises for large and excess concentrations of TDG, and it does not substantially alter catalytic activity.

TDG binding to a G•T mispair

The anisotropy and EMSA data for TDG binding to 16T^{F}11, a G•T substrate analog that can accommodate 2:1 binding, are shown in Figure 4A and B. Inspection of the anisotropy data suggests two nonequivalent sites, and fitting to a two-site model reveals tight binding of one TDG subunit to the G•T^F site, K_{d1} = 18 ± 3 nM, and weak binding of a second TDG subunit to give a 2:1 complex, K_{d2} = 1279 ± 279 nM. The total change in anisotropy (Δr = 0.090) is nearly identical to that observed for

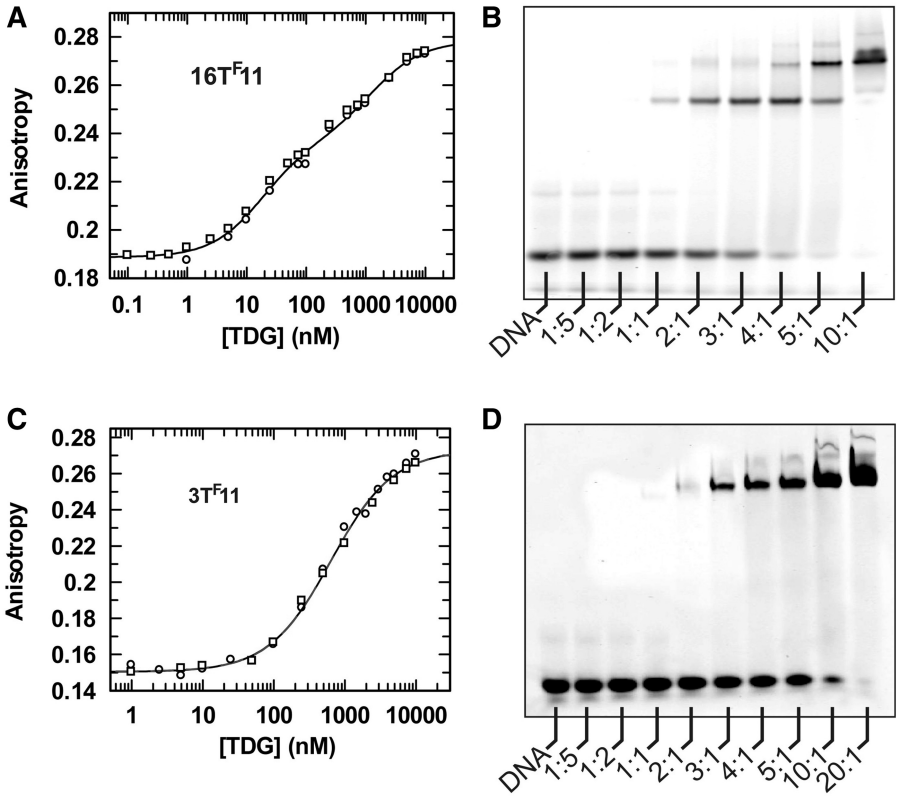

Figure 4. TDG binding to G•T^F substrate analogs monitored by fluorescence anisotropy and EMSAs. (**A**) Anisotropy data for equilibrium binding of TDG to 16T^{F}11 (0.5 nM), obtained from two independent experiments (open circle, open rectangle). Fitting to a two-site binding model gives $K_{d1} = 18 \pm 3$ nM, and $K_{d2} = 1279 \pm 279$ nM (and anisotropy of $r_D = 0.189$, $r_{ED} = 0.237$, $r_{EED} = 0.278$). (**B**) EMSA for TDG binding to 16T^{F}11 (0.5 uM); the [TDG]:[DNA] ratio is indicated. (**C**) Anisotropy data for TDG binding to 3T^{F}11 (0.5 nM) obtained from two independent experiments (open circle, open rectangle). Fitting to a two-site model gives $K_{d1} = 124 \pm 25$ nM, and $K_{d2} = 818 \pm 80$ nM (and $r_D = 0.150$, $r_{ED} = 0.176$, $r_{EED} = 0.273$). To obtain a proper fit it was necessary to fix $r_{ED} = 0.176$, which is based on $r_D = 0.150$ (fitted for 3T^{F}11) and Δr for 1:1 binding to 3U^{F}11 ($\Delta r_{1:1} = r_{ED} - r_D = 0.026$). (If r_{ED} is not fixed, K_{d2} and r_{EED} are poorly constrained and unreasonably high). The data are better fitted to a two-site rather than one-site binding model ($P = 0.011$). Moreover, 2:1 binding to 3T^{F}11 is indicated by observation that the total anisotropy change is slightly larger for 3T^{F}11 ($r_{EED} - r_D = \Delta r_{tot} = 0.123$) than for 3U^{F}11 ($\Delta r_{tot} = 0.103$), for which 2:1 binding is demonstrated by anisotropy and EMSA. (**D**) EMSA for TDG binding to 3T^{F}11 (0.5 uM). Low population of the 2:1 complex at the highest TDG:DNA ratio is likely due to dissociation during electrophore2sis, as 3T^{F}11 exhibits very rapid dissociation (k_{off}) from TDG (unpublished data).

16U^{F}11 ($\Delta r = 0.093$). The EMSA for TDG binding to 16T^{F}11 confirms 1:1 binding at lower TDG:DNA ratios and 2:1 binding at high TDG concentrations. The anisotropy data for TDG binding to 3T^{F}11 (Figure 4C), which cannot accommodate 2:1 binding (crystallographic), indicates relatively tight binding to the G•T site, $K_{d1} = 124 \pm 25$ nM, and weak binding of a second TDG subunit, $K_{d2} = 818 \pm 80$ nM, to give an alternate 2:1 complex. The EMSA for TDG binding to 3T^{F}11 is consistent with this binding stoichiometry (Figure 4D). The relatively tight binding of TDG to 3T^{F}11 shows the 2:1 complex in the crystal structure is not required for specific binding of TDG to a G•T mispair.

2:1 binding is not required for G•T repair activity

Our results indicate 2:1 binding to G•T mispairs is highly unlikely under limiting enzyme conditions, because K_{d2} is weak, and $K_{d2} >> K_{d1}$. Nevertheless, we sought to determine whether 2:1 binding, if it occurs, could enhance catalytic activity for G•T substrates. We showed previously that 2:1 binding is dispensable for G•U activity (18), but the result could potentially differ for G•T activity, since binding and catalysis is much weaker for G•T relative to G•U substrates (Table 1) (19,22). We used single turnover kinetics experiments with saturating TDG (5000 nM) and limiting G•T substrate (500 nM) such that 2:1 binding predominates. As shown in Figure 5A, the maximal rate of base excision is the same for a G•T substrate that can accommodate 2:1 binding ($k_{max} = 0.16 \pm 0.03\ min^{-1}$) and one that cannot ($k_{max} = 0.14 \pm 0.03\ min^{-1}$). We conclude 2:1 binding does not enhance catalytic activity for G•T substrates.

We also approached this question using pre-steady-state multiple turnover kinetics, collected with saturating G•T substrate (2000 nM) and limiting TDG (200 nM), such that 2:1 binding is negligible (Figure 5B). Under these conditions, TDG exhibits an exponential phase, $k_{obs} = 0.12 \pm 0.02\ min^{-1}$, reflecting the maximal rate of base excision, followed by a much slower steady-state

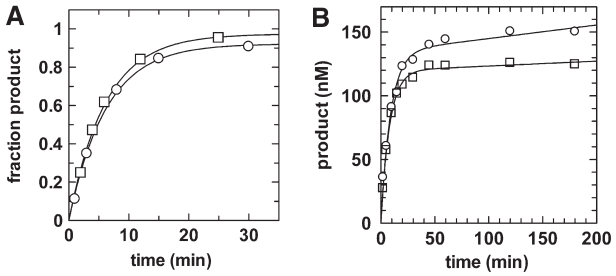

Figure 5. Kinetics experiments show 2:1 binding is not needed for processing G•T substrates. (**A**) Single turnover kinetics collected with saturating TDG (5000 nM) and limiting G•T substrate (500 nM), one of which can accommodate 2:1 binding (16T11, open circle) and one that cannot (4T11, open rectangle). Fitting the data (multiple experiments) to Equation (1) gives $k_{max} = 0.16 \pm 0.03\,min^{-1}$ (16T11) and $k_{max} = 0.14 \pm 0.03\,min^{-1}$ (4T11). We note that 4T11 is the minimal DNA construct that provides full G•T activity, due likely to non-specific interactions between the DNA (5′ of the dT target) and the N-terminal region of TDG (unpublished data). However, 4T11 still lacks the entire binding site for the second TDG subunit as seen in the crystal structure (Figure 1). (**B**) Pre-steady-state multiple-turnover kinetics collected with saturating G•T substrate (2000 nM) and limiting TDG (200 nM). Fitting the data (multiple experiments) for 16T11 (open circle) to Equation (2) gives a rate constant of $k_{obs} = 0.12 \pm 0.02\,min^{-1}$ and amplitude $A = 134 \pm 3$ nM for the exponential phase, and a rate constant of $k_{cat} = 0.0006 \pm 0.0003\,min^{-1}$ for the steady-state phase. The parameters are very similar for 4T11 (open rectangle); $k_{obs} = 0.12 \pm 0.02\,min^{-1}$, $A = 117 \pm 3$ nM, and $k_{cat} = 0.0002 \pm 0.0001\,min^{-1}$. Observation of slightly greater amplitude for 16T11 indicates 1:1 binding to both substrates, because 4T11 cannot accommodate 2:1 binding, consistent with other results above. For G•T substrates, we typically find $A <$ [TDG]. However, for G•U and G•FU substrates, we find $A = \sim$[TDG], indicating TDG is fully active (Supplementary Figure S1). We are currently investigating the basis of the diminished amplitude for G•T substrates. However, this does not alter our conclusion that 2:1 binding is not needed for G•T activity.

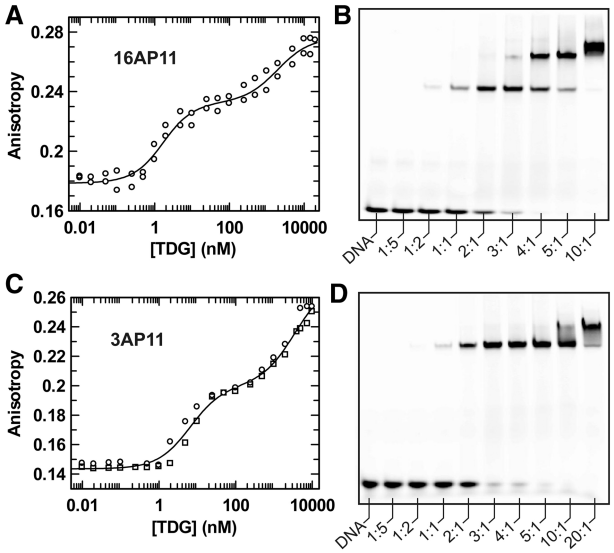

Figure 6. TDG binding to abasic (AP) DNA product monitored by fluorescence anisotropy and EMSA. (**A**) Anisotropy data for equilibrium binding of TDG to 16AP11 (0.5 nM). Fitting to a two-site binding model gives $K_{d1} = 1.4 \pm 0.4$ nM and $K_{d2} = 1926 \pm 762$ nM (and anisotropy of $r_D = 0.178$, $r_{ED} = 0.233$, $r_{EED} = 0.276$). Due to slow dissociation of AP DNA from TDG, the anisotropy data were collected using individual samples that were incubated for at least 2 h prior to data collection to ensure equilibration. Our unpublished data by stopped-flow and other kinetic methods show 2 h is sufficient for equilibration (confirmed in some cases by repeating measurements after additional equilibration time). (**B**) EMSA for TDG binding to 16AP11 (0.5 uM), with the [TDG]:[DNA] ratio indicated. (**C**) Anisotropy data for TDG binding to 3AP11 (0.5 nM) obtained from two independent experiments (open circle, open rectangle). Fitting to a two-site binding model gives $K_{d1} = 6.2 \pm 1.3$ nM and $K_{d2} = 3480 \pm 1173$ nM (and anisotropy of $r_D = 0.144$, $r_{ED} = 0.200$ and $r_{EED} = 0.271$). (**D**) EMSA for TDG binding to 3AP11 (0.5 uM).

phase (33). Observation that the maximal base excision rate is nearly the same for conditions of saturating TDG or saturating G•T substrate confirms that 2:1 binding, if it occurs, does not substantially enhance G•T activity.

TDG binding to abasic DNA product

It is also important to determine the stoichiometry and affinity for TDG binding to its abasic (or AP) DNA product. Anisotropy data for TDG binding to 16AP11 DNA, which contains a G•AP site and is long enough to accommodate 2:1 binding, are shown in Figure 6A. The anisotropy data indicate two nonequivalent sites, and fitting to a two-site model reveals tight binding of one TDG subunit to the AP site, $K_{d1} = 1.4 \pm 0.4$ nM and very weak binding of a second TDG subunit to give a 2:1 complex, $K_{d2} = 1926 \pm 762$ nM. The EMSA for TDG binding to 16AP11 (Figure 6B) confirms the binding stoichiometry indicated by anisotropy; 1:1 binding at lower TDG:DNA ratios and 2:1 binding for large and excess TDG concentrations.

Anisotropy data for TDG binding to 3AP11 indicates relatively tight binding to the G•AP site, $K_{d1} = 6.2 \pm 1.3$ nM, and very weak binding of a second TDG subunit to give an alternate 2:1 complex, $K_{d2} = 3480 \pm 1173$ nM (Figure 6C). The stoichiometry and relative affinities indicated by the anisotropy experiments are qualitatively confirmed by an EMSA (Figure 6D). The tight binding of a single TDG subunit to 3AP11 shows that a second TDG subunit is not required for specific binding to a G•AP product site.

TDG binding to an undamaged CpG site

It is known that TDG is specific for G•T mispairs and other lesions located in a CpG sequence context (19,21,23,46), but the affinity of TDG for an undamaged CpG site had not been determined. Such knowledge is important for understanding how TDG locates G•T mispairs arising at CpG sites and its role(s) in transcriptional regulation. We previously showed TDG exhibits exceedingly low activity for cleaving cytosine from a CpG site (<1% product in 8 h), thus binding studies can be performed in the absence of base cleavage (24). Anisotropy and EMSA data for TDG binding to 28-bp DNA containing a CpG site (16C11) are shown in Figure 7A and 7B. The anisotropy data indicate that TDG binds the CpG site with remarkably tight affinity, $K_{d1} = 63 \pm 10$ nM, and a second TDG subunit binds with much weaker affinity, $K_{d2} = 965 \pm 148$ nM, at high TDG concentrations. The EMSA confirms the stoichiometry indicated by the anisotropy data.

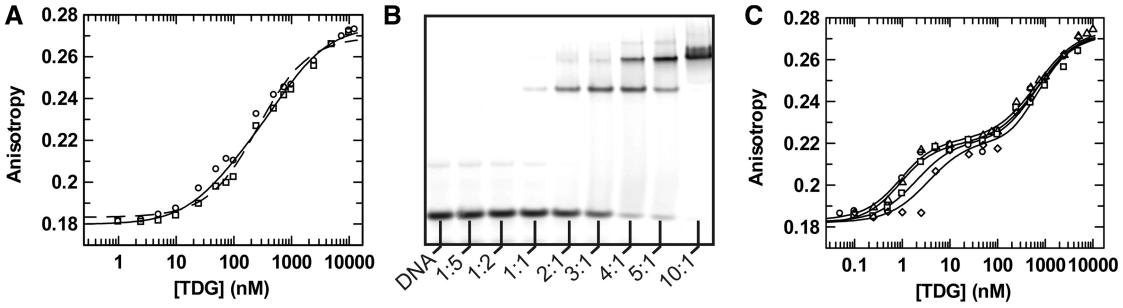

Figure 7. TDG binding to DNA containing a single CpG site, monitored by fluorescence anisotropy and an EMSA. (**A**) Anisotropy data for equilibrium binding of TDG to the 28-bp 16C11 DNA (0.5 nM) obtained from two independent experiments (open circle, open rectangle). Fitting to a two-site binding model gives $K_{d1} = 63 \pm 10$ nM, and $K_{d2} = 965 \pm 148$ nM (and anisotropy of $r_D = 0.180$, $r_{ED} = 0.223$, $r_{EED} = 0.275$). To obtain a good fit, it was necessary to fix $r_{ED} = 0.223$. This value is the sum of $r_D = 0.180$ (fitted for 16C11) and $\Delta r_{1:1} = 0.043$ (average of $\Delta r_{1:1}$ values for $16U^F11$ and $16T^F11$). Otherwise, the fitted r_{ED} is unreasonably high (0.25), and K_{d2} and r_{EED} are poorly constrained. The data are better fitted to model for two-site versus one-site binding (dashed line, $P = 0.010$). (**B**) EMSA for TDG binding to 16C11 (0.5 uM), with the [TDG]:[DNA] ratios given. (**C**) Equilibrium competition anisotropy experiments for TDG binding to TR-labeled $16U^F11$ (0.5 nM) collected in the absence of 16C11 (open circle and open triangle, data from Figure 3B) and in the presence of 16C11 at a concentration of 50 nM (open rectangle) or 125 nM (open rhombus). The data were fitted globally to model with two TDG binding sites for $16U^F11$ and 16C11, giving $K_{d1} = 26 \pm 8$ nM for 16C11, and $K_{d1} = 0.59 \pm 0.14$ nM and $K_{d2} = 673 \pm 100$ nM for $16U^F11$ (anisotropy for $16U^F11$ of $r_D = 0.182$, $r_{ED} = 0.221$, $r_{EED} = 0.274$). K_{d2} for 16C11 is poorly constrained by the data (and unreasonably large). Fitting the data to a competition model with one site for 16C11 gives the same K_{d1} (within error). However, the data in (A) and (B) show TDG can form a 2:1 complex with 16C11.

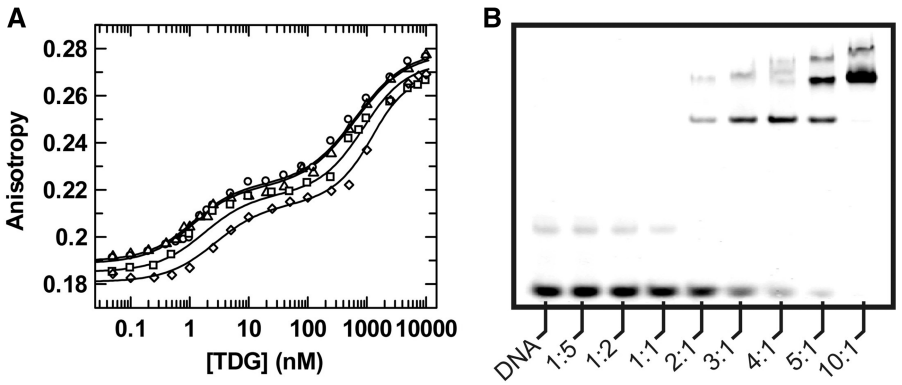

Figure 8. TDG binding to nonspecific DNA monitored fluorescence anisotropy and an EMSA. (**A**) Equilibrium competition anisotropy experiments for TDG binding to TR-labeled $16U^F11$ (0.5 nM) collected in the absence of NS28 (open circle, open triangle) and with NS28 concentrations of 200 nM (open rectangle) or 500 nM (open rhombus). Global fitting of all data to model involving two TDG binding sites for $16U^F11$ and two equivalent and independent sites for NS28 (i.e. restrained to $K_{d2} = 4*K_{d1}$) gives $K_{d1} = 293 \pm 64$ nM and $K_{d2} = 1172 \pm 254$ nM for NS28. For $16U^F11$, the fitting gives $K_{d1} = 0.88 \pm 0.13$ nM and $K_{d2} = 654 \pm 62$ nM (and anisotropy of $r_D = 0.189$, $r_{ED} = 0.221$, $r_{EED} = 0.278$). Fitting the data to a model involving a single site for NS28 gives essentially the same result for NS28 binding, $K_{d1} = 279 \pm 69$ nM, and for the $16U^F11$ parameters (data not shown). (**B**) EMSA for TDG binding to 28 bp nonspecific DNA (NS28, 0.5 uM) with the [TDG]:[DNA] ratio indicated.

To obtain another measure of TDG affinity for an undamaged CpG site, we performed equilibrium competition experiments, by collecting anisotropy data for TDG binding to $16U^F11$ (labeled) in the presence of two different concentrations of unlabeled 16C11 (Figure 7C). Global fitting of all the data to a model describing two TDG binding sites for $16U^F11$ and 16C11 gives $K_{d1} = 26 \pm 8$ nM for 1:1 binding to 16C11, but K_{d2} is poorly constrained by the data (and unreasonably large). The global fitting provides another measure of TDG affinity for $16U^F11$ in the presence of a DNA competitor, giving dissociation constants identical to those obtained in the absence of 16C11. Our results show TDG binds tightly to undamaged CpG sites, with an affinity that is merely 4-fold lower than for G•T mispairs.

TDG binding to nonspecific DNA

To gain perspective on the binding affinity of the second TDG subunit (K_{d2}) of the 2:1 complex, which binds a nonspecific region of DNA (Figure 1), we determined the affinity of TDG for binding DNA that is entirely nonspecific (contains no mispair or CpG site). We determined the affinity of TDG for 28-bp nonspecific DNA (NS28) using equilibrium competition binding experiments, by collecting anisotropy data for TDG binding to $16U^F11$ (labeled) in the presence of fixed concentrations of unlabeled NS28 (Figure 8A). Global fitting of data collected in the presence and absence of NS28 to a competitive model describing two binding sites for $16U^F11$ and two equivalent and independent binding sites for NS28

(i.e. restrained to $K_{d2} = 4*K_{d1}$) gives $K_{d1} = 293 \pm 64$ nM and $K_{d2} = 1172 \pm 254$ nM. The latter value falls in the range of K_{d2} values for other DNAs examined here (Table 1). Fitting the data to a model with just one site for NS28 gives essentially the same result, $K_{d1} = 279 \pm 69$ nM. However, the two-site model is consistent with a binding analysis by EMSA (Figure 8B), which shows a 1:1 complex at lower [TDG]/[NS28] ratios and a 2:1 complex for large and excess TDG concentrations. Global fitting of the data in Figure 8A also provides a measure of TDG affinity for $16U^F11$ in the presence of nonspecific DNA, and gives essentially the same dissociation constants as obtained in the absence of NS28. Our findings show TDG possesses substantial affinity for nonspecific DNA.

DISCUSSION

The remarkable observation from previous structural and biochemical studies that TDG can bind abasic DNA with 1:1 or 2:1 stoichiometry (18) raised the important questions of whether 2:1 binding contributes to the ability of TDG to find and initiate the repair of G•T and G•U lesions or to the mechanism by which APE1 stimulates TDG activity. We investigated these questions by determining the stoichiometry and affinity for TDG binding to a G•U or G•T substrate analog, an abasic site, an undamaged CpG site, and to nonspecific DNA.

Our findings provide insight into how TDG recognizes and processes G•U mispairs. TDG forms a very tight 1:1 complex with a G•U mispair ($K_{d1} = 0.6$ nM, Table 1), and a second subunit can bind with much weaker affinity ($K_{d2} = 660$ nM) for high concentrations of TDG that are in great excess over G•U DNA. The tight binding to a G•U mispair observed here is consistent with previous results using DNA containing a $G•U^F$ analog (26). TDG also binds tightly to $3U^F11$ ($K_d = 8$ nM), showing the 2:1 complex observed in the TDG crystal structure is not needed for specific recognition of a G•U mispair. This is consistent with our previous kinetics experiments showing 1:1 binding provides full G•U catalytic activity (18). The 1000-fold difference in binding affinity for the two sites of the 2:1 complex, and the weak affinity of the second site relative to nonspecific DNA (NS28), indicates that under conditions of limiting enzyme and a huge excess of nonspecific DNA, TDG processes G•U lesions with 1:1 stoichiometry. This conclusion is supported by previous footprinting experiments, which indicated 1:1 binding to DNA containing a $G•U^F$ analog under conditions of limiting TDG (26). However, given that other glycosylases process G•U lesions much more efficiently than TDG, the more relevant question is whether 2:1 binding contributes to repair of G•T lesions, the primary biological target of TDG.

Our results indicate that TDG also binds and processes G•T lesions with 1:1 stoichiometry. TDG binds tightly to 28 bp DNA containing a G•T substrate analog ($K_{d1} = 18$ nM), and a second subunit binds with much weaker affinity ($K_{d2} = 1280$ nM) for large and excess concentrations of TDG. The large difference in affinity for the two sites ($K_{d2}/K_{d1} = 71$) and the weak affinity of TDG for the second site (K_{d2}) relative to nonspecific DNA indicates 2:1 binding to G•T mispairs is unlikely for cellular conditions of limiting TDG and a large excess of nonspecific DNA. Moreover, the relatively tight affinity of TDG for $3T^F11$ indicates the 2:1 complex is not needed for specific recognition of G•T lesions. Finally, our kinetics experiments show that 1:1 binding provides full catalytic activity for G•T processing.

We find TDG binds a G•T mispair with about 30-fold weaker affinity than a G•U mispair. This is likely explained by the methyl group at C5 of thymine (uracil has hydrogen at C5), which may diminish the lifetime of the dT nucleotide in the flipped state due to steric hindrance in the TDG active site, as suggested by our previous kinetics results (21,22,24). Given that G•T lesions arising at CpG sites are likely the predominant biological target of TDG (21,23), one might expect TDG to have evolved to bind more tightly to G•T mispairs. The weaker affinity for G•T mispairs may reflect a compromise between the competing needs for efficient processing of G•T lesions and avoiding the excision of T from the huge excess of A•T base pairs, which is governed in part by the 18 000-fold specificity of TDG for excising T from G•T versus A•T pairs (21).

Previous studies show TDG binds tightly to its AP DNA product, and that AP DNA is a potent inhibitor of the TDG reaction (32,33,47). Our anisotropy results here show TDG forms a very tight 1:1 complex with its reaction product, a G•AP site ($K_{d1} = 1.4$ nM), and a second subunit binds with much weaker affinity ($K_{d2} = 1.9$ μM) for large and excess concentrations of TDG. The huge difference in affinity for the two sites ($K_{d2}/K_{d1} = 1376$) and the weak affinity of TDG for the second site (K_{d2}) relative to nonspecific DNA indicates 2:1 binding to abasic sites is unlikely for cellular conditions of limiting TDG and excess nonspecific DNA. The conclusion that a second TDG subunit is not needed for tight binding to G•AP sites is supported by the high affinity of TDG for 3AP11 ($K_{d1} = 6$ nM).

Our findings have important implications for the stimulation of TDG activity by the follow-on base excision repair enzyme, APE1 (32). We previously showed that APE1 greatly enhances TDG activity, increasing its rate of steady-state turnover (k_{cat}) by 42- and 26-fold for G•T and G•U substrates, respectively (33). Our results here indicate that under the conditions used for these previous studies, limiting concentrations of TDG (and APE1) and a saturating amount of TDG substrate, TDG binds its product with 1:1 stoichiometry. Thus, the stimulatory effect of APE1 does not involve a TDG product complex with 2:1 stoichiometry. Consistent with this conclusion, we previously observed potent stimulation of TDG by APE1 for a short DNA that cannot accommodate two TDG subunits (3U12 substrate or 3AP12 product) (33). Together, these studies indicate the stimulatory effect of APE1 involves a TDG product complex with 1:1 stoichiometry.

The affinity of TDG for an undamaged CpG site had not been quantitatively examined, despite the strong specificity of TDG for G•T mispairs (and other

lesions) that are located in a CpG sequence context. We find TDG binds DNA containing a CpG site (16C11) with remarkable affinity, K_{d1} = 63 nM, about 4-fold weaker than its affinity for the same DNA containing a G•T lesion (Table 1). The specificity for a CpG site is also indicated by observation that TDG binds 4-fold tighter to 16C11 than to nonspecific DNA (NS28) that contains no CpG site but is otherwise identical. On an experimental note, our findings indicate that studies of TDG binding to a particular site (i.e. a G•T mispair) should use DNA that does not contain an undamaged CpG site.

Preferential binding to CpG requires a mechanism for recognizing these sites within a large background of nonspecific DNA. Previous studies suggest TDG may accomplish this by transiently flipping 2′-deoxycytidine (dC) out of a CpG site and into its active site (or flipping it partially into the active site). Our crystal structure indicates specificity for excising lesions from a CpG site involves interactions with the 3′-guanine (5′-XpG, X = lesion) that cannot be formed in the absence of nucleotide flipping (18), which suggests nucleotide (dC) flipping may be required for recognizing undamaged CpG sites. The ability of TDG to flip dC into its active site is indicated by our previous finding that TDG can cleave analogs of dC that have a weakened *N*-glycosylic bond (e.g. 5-fluoro-dC, 5-hydroxy-dC, etc.) (24). However, these results do not rule out a mechanism whereby TDG recognizes CpG sites in the absence of nucleotide flipping. Further studies are needed to resolve this question.

The ability of TDG to bind CpG sites and transiently flip dC into its active site, suggested by the findings herein and in our previous studies, may be important in the search for G•T lesions arising from deamination of m^5C, a modified base found selectively at CpG sites. In addition, the affinity of TDG for undamaged CpG sites and nonspecific DNA may be important for its ability to modulate the activity of transcription factors including retinoic acid and retinoid X receptors (48), estrogen receptor α (49) and thyroid transcription factor 1 (50), and co-activators such as CBP/p300 (51). Additional studies are needed to explore these ideas further.

In summary, we find TDG binds tightly to G•U and G•T mispairs, with subnanomolar and low nanomolar affinity, respectively, and that 1:1 binding provides full G•T repair activity. TDG forms a very tight 1:1 complex with abasic (G•AP) sites, indicating the stimulatory effect of APE1 does not require 2:1 binding of TDG to its product. TDG binds tightly to undamaged CpG sites, about 4-fold weaker than to G•T mispairs, and it exhibits substantial affinity for nonspecific DNA. While 2:1 binding to DNA is observed *in vitro* for large and excess concentrations of TDG, our results indicate that a single TDG subunit is fully capable of finding and processing G•U and G•T lesions.

SUPPLEMENTARY DATA

Supplementary Data are available at NAR Online.

ACKNOWLEDGEMENTS

We thank Petr Kuzmic for assistance with DynaFit, Jim Stivers (Johns Hopkins University) for providing purified human uracil DNA glycosylase, L. Eisele (NY State Department of Health) for collecting sedimentation velocity analytical ultracentrifugation data and the reviewers for excellent suggestions.

FUNDING

The National Institutes of Health (R01-GM-072711). Funding for open access charge: National Institutes of Health, USA.

Conflict of interest statement. None declared.

REFERENCES

1. Rideout,W.M. 3rd, Coetzee,G.A., Olumi,A.F. and Jones,P.A. (1990) 5-Methylcytosine as an endogenous mutagen in the human LDL receptor and p53 genes. *Science*, **249**, 1288–1290.
2. Cooper,D.N. and Youssoufian,H. (1988) The CpG dinucleotide and human genetic disease. *Hum. Genet.*, **78**, 151–155.
3. Sjoblom,T., Jones,S., Wood,L.D., Parsons,D.W., Lin,J., Barber,T.D., Mandelker,D., Leary,R.J., Ptak,J., Silliman,N. *et al.* (2006) The consensus coding sequences of human breast and colorectal cancers. *Science*, **314**, 268–274.
4. Pfeifer,G.P. and Besaratinia,A. (2009) Mutational spectra of human cancer. *Hum Genet*, **125**, 493–506.
5. Wiebauer,K. and Jiricny,J. (1990) Mismatch-specific thymine DNA glycosylase and DNA polymerase beta mediate the correction of G.T mispairs in nuclear extracts from human cells. *Proc. Natl Acad. Sci. USA*, **87**, 5842–5845.
6. Wiebauer,K. and Jiricny,J. (1989) In vitro correction of G.T mispairs to G.C pairs in nuclear extracts from human cells. *Nature*, **339**, 234–236.
7. Bellacosa,A., Cicchillitti,L., Schepis,F., Riccio,A., Yeung,A.T., Matsumoto,Y., Golemis,E.A., Genuardi,M. and Neri,G. (1999) MED1, a novel human methyl-CpG-binding endonuclease, interacts with DNA mismatch repair protein MLH1. *Proc. Natl Acad. Sci. USA*, **96**, 3969–3974.
8. Hendrich,B., Hardeland,U., Ng,H.H., Jiricny,J. and Bird,A. (1999) The thymine glycosylase MBD4 can bind to the product of deamination at methylated CpG sites. *Nature*, **401**, 301–304.
9. Klose,R.J. and Bird,A.P. (2006) Genomic DNA methylation: the mark and its mediators. *Trends Biochem. Sci.*, **31**, 89–97.
10. Hajkova,P., Jeffries,S.J., Lee,C., Miller,N., Jackson,S.P. and Surani,M.A. (2010) Genome-wide reprogramming in the mouse germ line entails the base excision repair pathway. *Science*, **329**, 78–82.
11. Wossidlo,M., Arand,J., Sebastiano,V., Lepikhov,K., Boiani,M., Reinhardt,R., Scholer,H. and Walter,J. (2010) Dynamic link of DNA demethylation, DNA strand breaks and repair in mouse zygotes. *EMBO J.*, **29**, 1877–1888.
12. Bhutani,N., Brady,J.J., Damian,M., Sacco,A., Corbel,S.Y. and Blau,H.M. (2010) Reprogramming towards pluripotency requires AID-dependent DNA demethylation. *Nature*, **463**, 1042–1047.
13. Popp,C., Dean,W., Feng,S., Cokus,S.J., Andrews,S., Pellegrini,M., Jacobsen,S.E. and Reik,W. (2010) Genome-wide erasure of DNA methylation in mouse primordial germ cells is affected by AID deficiency. *Nature*, **463**, 1101–1105.
14. Metivier,R., Gallais,R., Tiffoche,C., Le Peron,C., Jurkowska,R.Z., Carmouche,R.P., Ibberson,D., Barath,P., Demay,F., Reid,G. *et al.* (2008) Cyclical DNA methylation of a transcriptionally active promoter. *Nature*, **452**, 45–50.
15. Kangaspeska,S., Stride,B., Metivier,R., Polycarpou-Schwarz,M., Ibberson,D., Carmouche,R.P., Benes,V., Gannon,F. and Reid,G.

(2008) Transient cyclical methylation of promoter DNA. *Nature*, **452**, 112–115.
16. Jost,J.P., Schwarz,S., Hess,D., Angliker,H., Fuller-Pace,F.V., Stahl,H., Thiry,S. and Siegmann,M. (1999) A chicken embryo protein related to the mammalian DEAD box protein p68 is tightly associated with the highly purified protein–RNA complex of 5-MeC-DNA glycosylase. *Nucleic Acids Res.*, **27**, 3245–3252.
17. Cortazar,D., Kunz,C., Saito,Y., Steinacher,R. and Schar,P. (2007) The enigmatic thymine DNA glycosylase. *DNA Repair*, **6**, 489–504.
18. Maiti,A., Morgan,M.T., Pozharski,E. and Drohat,A.C. (2008) Crystal structure of human thymine DNA glycosylase bound to DNA elucidates sequence-specific mismatch recognition. *Proc. Natl Acad. Sci. USA*, **105**, 8890–8895.
19. Waters,T.R. and Swann,P.F. (1998) Kinetics of the action of thymine DNA glycosylase. *J. Biol. Chem.*, **273**, 20007–20014.
20. Hardeland,U., Bentele,M., Jiricny,J. and Schar,P. (2000) Separating substrate recognition from base hydrolysis in human thymine DNA glycosylase by mutational analysis. *J. Biol. Chem.*, **275**, 33449–33456.
21. Morgan,M.T., Bennett,M.T. and Drohat,A.C. (2007) Excision of 5-halogenated uracils by human thymine DNA glycosylase: robust activity for DNA contexts other than CpG. *J. Biol. Chem.*, **282**, 27578–27586.
22. Maiti,A., Morgan,M.T. and Drohat,A.C. (2009) Role of two strictly conserved residues in nucleotide flipping and N-glycosylic bond cleavage by human thymine DNA glycosylase. *J. Biol. Chem.*, **284**, 36680–36688.
23. Abu,M. and Waters,T.R. (2003) The main role of human thymine-DNA glycosylase is removal of thymine produced by deamination of 5-methylcytosine and not removal of ethenocytosine. *J. Biol. Chem.*, **278**, 8739–8744.
24. Bennett,M.T., Rodgers,M.T., Hebert,A.S., Ruslander,L.E., Eisele,L. and Drohat,A.C. (2006) Specificity of human thymine DNA glycosylase depends on N-glycosidic bond stability. *J. Am. Chem. Soc.*, **128**, 12510–12519.
25. Steinacher,R. and Schar,P. (2005) Functionality of human thymine DNA glycosylase requires SUMO-regulated changes in protein conformation. *Curr. Biol.*, **15**, 616–623.
26. Scharer,O.D., Kawate,T., Gallinari,P., Jiricny,J. and Verdine,G.L. (1997) Investigation of the mechanisms of DNA binding of the human G/T glycosylase using designed inhibitors. *Proc. Natl Acad. Sci. USA*, **94**, 4878–4883.
27. Barrett,T.E., Scharer,O.D., Savva,R., Brown,T., Jiricny,J., Verdine,G.L. and Pearl,L.H. (1999) Crystal structure of a thwarted mismatch glycosylase DNA repair complex. *EMBO J.*, **18**, 6599–6609.
28. Berger,I., Tereshko,V., Ikeda,H., Marquez,V. and Egli,M. (1998) Crystal structures of B-DNA with incorporated 2′-deoxy-2′-fluoro-arabino-furanosyl thymines: implications of conformational preorganization for duplex stability. *Nucleic Acids Res.*, **26**, 2473–2480.
29. Drohat,A.C., Jagadeesh,J., Ferguson,E. and Stivers,J.T. (1999) Role of electrophilic and general base catalysis in the mechanism of *Escherichia coli* uracil DNA glycosylase. *Biochemistry*, **38**, 11866–11875.
30. Jiang,Y.L., Ichikawa,Y. and Stivers,J.T. (2002) Inhibition of uracil DNA glycosylase by an oxacarbenium ion mimic. *Biochemistry*, **41**, 7116–7124.
31. Gill,S.C. and von Hippel,P.H. (1989) Calculation of protein extinction coefficients from amino acid sequence data. *Anal. Biochem.*, **182**, 319–326.
32. Waters,T.R., Gallinari,P., Jiricny,J. and Swann,P.F. (1999) Human thymine DNA glycosylase binds to apurinic sites in DNA but is displaced by human apurinic endonuclease 1. *J. Biol. Chem.*, **274**, 67–74.
33. Fitzgerald,M.E. and Drohat,A.C. (2008) Coordinating the initial steps of base excision repair. Apurinic/apyrimidinic endonuclease 1 actively stimulates thymine DNA glycosylase by disrupting the product complex. *J. Biol. Chem.*, **283**, 32680–32690.
34. Leatherbarrow,R.J. (1998) *Grafit 6*, Erithacus Software Ltd. Staines, UK.
35. Perez-Howard,G.M., Weil,P.A. and Beechem,J.M. (1995) Yeast TATA binding protein interaction with DNA: fluorescence determination of oligomeric state, equilibrium binding, on-rate, and dissociation kinetics. *Biochemistry*, **34**, 8005–8017.
36. Unruh,J.R., Gokulrangan,G., Wilson,G.S. and Johnson,C.K. (2005) Fluorescence properties of fluorescein, tetramethylrhodamine and Texas Red linked to a DNA aptamer. *Photochem. Photobiol.*, **81**, 682–690.
37. Unruh,J.R., Gokulrangan,G., Lushington,G.H., Johnson,C.K. and Wilson,G.S. (2005) Orientational dynamics and dye–DNA interactions in a dye-labeled DNA aptamer. *Biophys. J.*, **88**, 3455–3465.
38. Kuzmic,P. (1996) Program DYNAFIT for the analysis of enzyme kinetic data: application to HIV proteinase. *Anal. Biochem.*, **237**, 260–273.
39. Kuzmic,P. (2009) DynaFit - a software package for enzymology. *Methods Enzymol.*, **467**, 247–280.
40. Bowman,B.R., Lee,S.M., Wang,S.Y. and Verdine,G.L. (2008) Structure of the E-coli DNA glycosylase AlkA bound to the ends of duplex DNA: A system for the structure determination of lesion-containing DNA. *Structure*, **16**, 1166–1174.
41. Lee,S., Bowman,B.R., Ueno,Y., Wang,S. and Verdine,G.L. (2008) Synthesis and structure of duplex DNA containing the genotoxic nucleobase lesion N7-methylguanine. *J. Am. Chem. Soc.*, **130**, 11570–11571.
42. Bloom,L.B., Turner,J., Kelman,Z., Beechem,J.M., O'Donnell,M. and Goodman,M.F. (1996) Dynamics of loading the beta sliding clamp of DNA polymerase III onto DNA. *J. Biol. Chem.*, **271**, 30699–30708.
43. Gokulrangan,G., Unruh,J.R., Holub,D.F., Ingram,B., Johnson,C.K. and Wilson,G.S. (2005) DNA aptamer-based bioanalysis of IgE by fluorescence anisotropy. *Anal. Chem.*, **77**, 1963–1970.
44. Guan,X., Madabushi,A., Chang,D.Y., Fitzgerald,M., Shi,G., Drohat,A.C. and Lu,A.L. (2007) The human checkpoint sensor Rad9-Rad1-Hus1 interacts with and stimulates DNA repair enzyme TDG glycosylase. *Nucleic Acids Res.*, **35**, 6207–6218.
45. Baba,D., Maita,N., Jee,J.-G., Uchimura,Y., Saitoh,H., Sugasawa,K., Hanaoka,F., Tochio,H., Hiroaki,H. and Shirakawa,M. (2005) Crystal structure of thymine DNA glycosylase conjugated to SUMO-1. *Nature*, **435**, 979–982.
46. Sibghat,U., Gallinari,P., Xu,Y.Z., Goodman,M.F., Bloom,L.B., Jiricny,J. and Day,R.S. III. (1996) Base analog and neighboring base effects on substrate specificity of recombinant human G:T mismatch-specific thymine DNA-glycosylase. *Biochemistry*, **35**, 12926–12932.
47. Scharer,O.D., Nash,H.M., Jiricny,J., Laval,J. and Verdine,G.L. (1998) Specific binding of a designed pyrrolidine abasic site analog to multiple DNA glycosylases. *J. Biol. Chem.*, **273**, 8592–8597.
48. Um,S., Harbers,M., Benecke,A., Pierrat,B., Losson,R. and Chambon,P. (1998) Retinoic acid receptors interact physically and functionally with the T:G mismatch-specific thymine-DNA glycosylase. *J. Biol. Chem.*, **273**, 20728–20736.
49. Chen,D., Lucey,M.J., Phoenix,F., Lopez-Garcia,J., Hart,S.M., Losson,R., Buluwela,L., Coombes,R.C., Chambon,P., Schar,P. *et al.* (2003) T:G mismatch-specific thymine-DNA glycosylase potentiates transcription of estrogen-regulated genes through direct interaction with estrogen receptor {alpha}. *J. Biol. Chem.*, **278**, 38586–38592.
50. Missero,C., Pirro,M.T., Simeone,S., Pischetola,M. and Di Lauro,R. (2001) The DNA glycosylase T:G mismatch-specific thymine DNA glycosylase represses thyroid transcription factor-1-activated transcription. *J. Biol. Chem.*, **276**, 33569–33575.
51. Tini,M., Benecke,A., Um,S.J., Torchia,J., Evans,R.M. and Chambon,P. (2002) Association of CBP/p300 acetylase and thymine DNA glycosylase links DNA repair and transcription. *Mol. Cell*, **9**, 265–277.